LA-UR-18-23419
Approved for public release; distribution is unlimited.

Title: Updated Erosion Analysis for Material Disposal Area G, Technical Area 54, Los Alamos National Laboratory

Author(s): Atchley, Adam Lee
Stauffer, Philip H.
Birdsell, Kay Hanson
Middleton, Richard Stephen

Intended for: Report

Issued: 2018-05-24 (rev.1)

LA-UR-18-23419

Updated Erosion Analysis for Material Disposal Area G, Technical Area 54, Los Alamos National Laboratory

Authors:
Adam L. Atchley, Philip H. Stauffer, Kay H. Birdsell, and Richard Middleton
Los Alamos National Laboratory

Prepared for:
U.S. Department of Energy

Date:
April 2018

Table of Contents

List of Figures

List of Tables

Acronyms and Abbreviations

CA	Composite Analysis
DEM	Digital Elevation Model
DOE	U.S. Department of Energy
HEM	Hillslope Erosion Model
IRS	Infiltration and Runoff Simulation
LEM	Landscape Evolution Model
LANL	Los Alamos National Laboratory
MDA G	Material Disposal Area G
NOAA	National Oceanic and Atmospheric Administration
PA	Performance Assessment
PA/CA	Performance Assessment and Composite Analysis
WEPP	Water Erosion Prediction Project

1.0 Introduction

Material Disposal Area G (MDA G), located within Technical Area 54 (TA-54) is used to dispose radioactive waste at Los Alamos National Laboratory (LANL). Technical Area 54 is located on LANL property on the Pajarito Plateau between the communities of Los Alamos and White Rock (Figure 1-1). The MDA G disposal facility is currently in operation (Figure 1-2). Waste is generally placed in large rectangular pits, numbered 1-39, and cylindrical shafts within MDA G.

U.S Department of Energy (DOE) Order 435.1 (DOE, 2001) requires that radioactive waste be managed in a manner that protects public health and safety and the environment. DOE facilities that receive waste after September 26, 1988, which includes MDA G, are therefore required to prepare and maintain a site-specific radiological performance assessment (PA). These sites are also required to conduct a composite analysis (CA) that accounts for the cumulative impacts of all waste that has been and will be disposed of at the facilities that includes other sources of radioactive material that may interact with these facilities. The PA/CA is required to assess the radiological impacts of the waste over a 1,000-year compliance period. This 1,000-year period begins after the expected site closer date (originally 2047 but recently modified to 2035).

LANL issued Revision 4 of the Area G performance assessment and composite analysis (PA/CA) in 2008 (LANL, 2008). The SIBERIA landscape evolution model (Willgoose and Riley, 1998) was applied to evaluate the impacts of surface erosion on the long-term performance of a final cover design adopted for those analyses (Wilson et al., 2005). The modeling was conducted using a version of SIBERIA (version 8.26) that was unable to account for changes in soil properties that may occur as successive layers of material are eroded from a site. Version 8.33 of SIBERIA, issued in 2006, added a "layers" model that implemented a method for tracking such changes. This version was used to update the MDA G surface erosion modeling; the results of this revision were reported in French and Crowell (2010). The erosion modeling reported in Wilson et al. (2005) and French and Crowell (2010) estimates patterns and rates of soil loss for three erosion scenarios –

low, moderate, and high – that differ in terms of runoff volume and ground surface characteristics. These scenarios were defined, in part, using average properties of 17 hillslope profiles located within, or immediately adjacent to, MDA G. Later, a sensitivity analysis was performed to evaluate a range of conditions observed across the 17 profiles (Crowell, 2013).

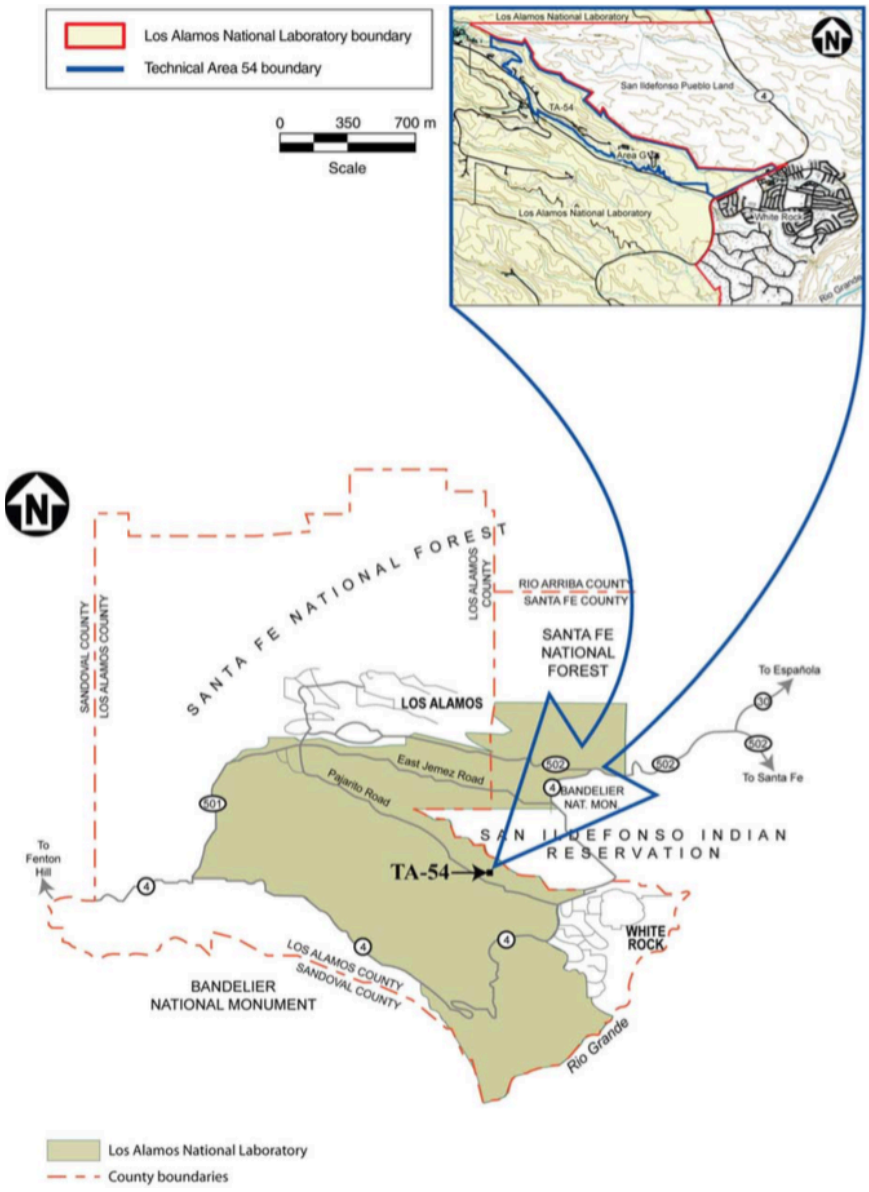

Figure 1-1. Location of MDA G with respect to the Laboratory and surrounding communities

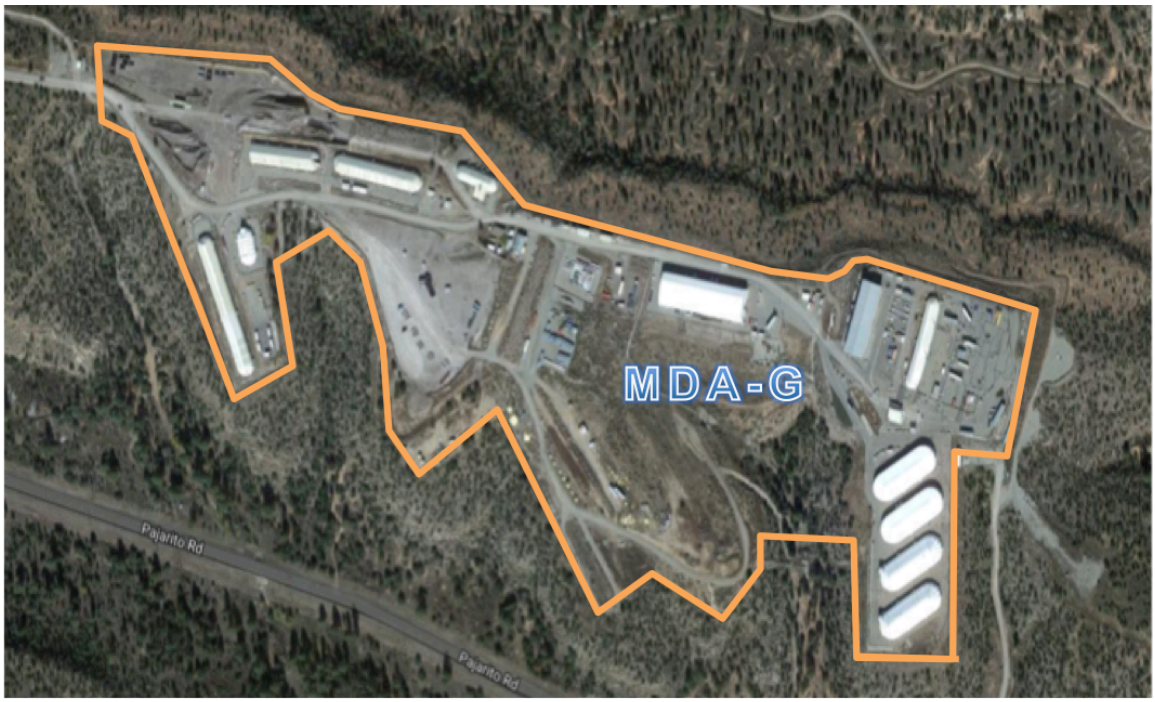

Figure 1-2. Site map of MDA G

All previous erosion studies for MDA G (Wilson et al., 2005; French and Crowell, 2010; Crowell, 2013) evaluated the cover performance over 1,000 years, which spans the required PA compliance period (DOE, 2001). However, it is acknowledged that radioactive material may interact with the surrounding environment beyond the passive institutional control period of 1,000 years. In fact, simulations for some groundwater transport scenarios have been conducted out to 100,000 years in order to evaluate full residence time distributions for breakthrough at the compliance point for the groundwater pathway (Stauffer et al., 2013). The work reported here extends the erosion analysis to 10,000 years to gain insight into potential for long-term erosion and to better understand the limitations of the analysis. Calculations of erosion provide estimates of mass removed; however at this time, the analysis has not been carried through to calculate exposure or dose impacts in the PA/CA site model. Within the PA/CA GoldSim model, SIBERIA results are used to project rates of soil loss through time across several disposal regions at MDA G; these losses are used to update the thickness of the surface soil, cap, and waste layers through time for each region. In addition, SIBERIA results are used in

the PA/CA model to assign sediment loads that are transport through time by erosion into catchments in the two neighboring canyons.

In this report, Section 2 describes the governing equations and fundamental assumptions of SIBERIA and the erosion modeling background as applied to MDA G, including the validation process and the resulting range of uncertainty. Section 3 presents the results of the extended 10,000-year analysis and compares results to the original 1,000-year analysis, demonstrates the role of armor at MDA G, and describes how uncertain model parameterization produced different landscape formation. Section 4 discusses how the uncertainty, model calibration, and model assumptions influence the extended erosion analysis and concludes with further steps that could improve erosion forecasting. Section 5 gives conclusions and discusses potential future work.

2.0 Background and Methods

The extended erosion analysis builds on a sensitivity analysis (Crowell 2013) and the original erosion modeling framework for MDA G (Wilson et al., 2005). SIBERIA is the central model used in the MDA G erosion analysis. A general description of SIBERIA is given in Section 2.1, which includes the governing equations and assumptions used in SIBERIA. Section 2.2 outlines the methods used in this study, including an in-depth description of the model parameterization, and describes how the MDA G erosion modeling framework is applied in this analysis. Much of the method description included here follows that of French and Crowell (2010), and Crowell (2013) where additional detail can be found.

2.1 Modeling Background

SIBERIA (Willgoose and Riley, 1998; Willgoose et al., 1991a; Willgoose, 2005) is in the class of erosion models known as landscape evolution models (LEM), which are designed to simulate the development of drainage networks and depositional features such as alluvial fans. In contrast to sediment transport models, such as the

Water Erosion Prediction Project (WEPP) (Laflen et al., 1991), KINEROS (Smith et al., 1995), and the Hillslope Erosion Model (HEM) (Lane et al., 2001), LEMs represent whole landscape features. LEMs further attempt to forecast how landscape features evolve over time by representing the lowering of ridges, incision or infilling of valleys and hollows, and the development of gullies and fans due to erosion, sediment transport, and material deposition. These processes alter and deform the terrain to produce an evolving three-dimensional (3D) representation of the landscape. As applied to MDA G, the SIBERIA modeling projects spatially variable rates of sediment transport and estimates spatial and temporal changes in the thickness of cover material remaining over the waste placed in the disposal pits and shafts.

SIBERIA is a simple form of LEM that considers erosion as a function of slope and the contributing area of runoff within a landscape feature. This simplicity allows SIBERIA to employ the 'geomorphically effective event assumption' that assumes, at long time scales, erosion can be represented as a steady process, and runoff is considered as a constant low-magnitude process that shapes the landscape. The 3D forecast of drainage networks and SIBERIA's computational efficacy enable long-time-scale simulations that are necessary for long-term erosion forecasts at MDA G.

2.1.1 Governing equations

SIBERIA simulates erosion and sediment transport over a landscape represented as a gridded digital elevation model (DEM). The erosion and sediment simulation deforms the model landscape over time. Sediment transport through each grid cell is calculated with an expression of the form:

$$Q_s = BA^mS^n + D_zS$$

Where

Q_s = sediment flux through a grid cell (kg/m width)

B = a coefficient that establishes the rate of sediment transport

A = area that contributes to runoff (m^2)

S = terrain slope (m/m)

m, n = exponents used to define how sediment yield depends on runoff contribution area (A) and slope (S) for a given cell

D_z = diffusion coefficient (kg/m width)

The exponents *m* and *n* affect the long-term form of the landscape, while the rate at which the landscape evolves through erosion is determined by the parameter *B*. The value of *B* is related to the short-term, event-based sediment flux through a scaling relationship with mean annual peak discharge and event duration provided in Willgoose (1989) and Willgoose et al. (1991a). D_z is the diffusion transport coefficient is a spatially constant Fickian diffusion term that is intended to represent the long-term average of the cumulative effects from hillslope soil creep, rainsplash, and rock-slide. Over time D_z will have a strong influence on the shape of the landform, where high D_z will result in soil movement from upslope areas resulting in high erosion fluxes.

Willgoose et al. (1991b) developed a relationship between local slope and contributing area with the form $S = cA^{-\alpha}$ where *c* is a constant and the scaling coefficient $\alpha = (m - 1)/n$. This relationship defines which processes dominate local erosion, the diffusion processes of soil creep and rainsplash or advection-dominated transport in channels. The log-log plot shown in Figure 2-1 demonstrates how small contributing areas, typical of the upper portions of hillslopes, are dominated by diffusion transport. The slope increases along flow paths within the diffusion-dominated region (Willgoose et al., 1991b). However, as contributing area grows, advection-driven erosion processes begin to dominate, and the effect of slope on processes like creep and inter-rill erosion diminishes. Advection-driven erosion then becomes dominant within channels where the larger contributing area provides more runoff for advection-dominated sediment transport, and the in-channel slope decreases with increased flow path lengths.

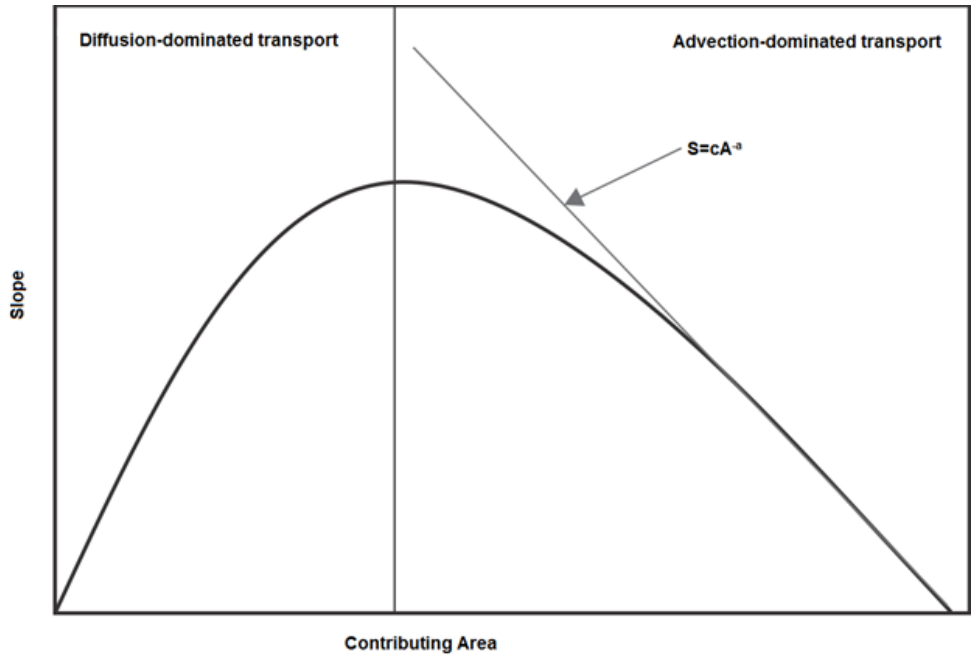

Figure 2-1. Area-slop plot illustrating dominate forms of erosion as a function of the slope area relationship. After Willgoose et al., (199b) and Crowell, (2013).

2.1.2 Model assumptions

Computational efficiency, and therefore ability to simulate long time scales, relies on the 'geomorphically effective runoff event' assumption. The assumption is that a single steady runoff rate is equivalent to a series of natural runoff events in terms of average sediment movement and geomorphic landform evolution. The geomorphically effective runoff event assumption has been justified by deriving a time-averaged sediment transport equation in which the representative discharge is equal to the mean annual peak discharge (Willgoose et al., 1998). However, the resulting representative discharge is noted as approximate and variability of runoff is lost (Tucker and Hancock, 2010). Instead of variable runoff intensities, the representative discharge for each cell is calculated as a function of the contributing drainage area and applied constantly through time. While this assumption allows for efficient computational time and long simulated time scales, the simplified flow propagation means that the effects of differential flow depths and varied flow velocities are not represented.

2.2 Methods

2.2.1 Model Parameterization & Validation

Building the MDA G erosion modeling framework necessitates a complex workflow to provide SIBERIA with realistic model parameters. If direct data are available, SIBERIA can be parameterized directly using long-term rainfall, runoff, and sediment yield data. Unfortunately, this is not the case for MDA G, and surrogate sites and reduced-order models were necessary for parameter estimation. Figure 2-2, shows the complete workflow for the MDA G erosion modeling framework. The majority of this section focuses on Branch 1, the steps that incorporate rainfall/runoff data to parameterize B, m, and n, and provide an initial estimate for D_z, as it is the most complicated and likely the largest source of model uncertainty. Section 2.2.2, briefly discusses Branch 3, assignment of the depth and location of bedrock layers and engineered armor in the form of placed boulders around the rim of the mesa. That is followed by a discussion of Branch 2, incorporating the central MDA G landform using a DEM.

To manage the workflow shown in Figure 2-2, including the stand-alone numerical codes used to parameterize SIBERIA, the entire workflow was streamlined using the Model Analysis Toolkit (MATK) wrapper function, which allows for all surrogate models and a SIBERIA forward run to be performed without manually transferring data. Each model run and associated parameters values are stored for reference and tracked by ensemble number. In addition, MATK allows for massively parallel ensemble sensitivity studies of desired variables, which govern erosion and gully formation. Sensitivity of all 70 SIBERIA parameters and domain configurations, such as estimated bedrock elevations, can be made.

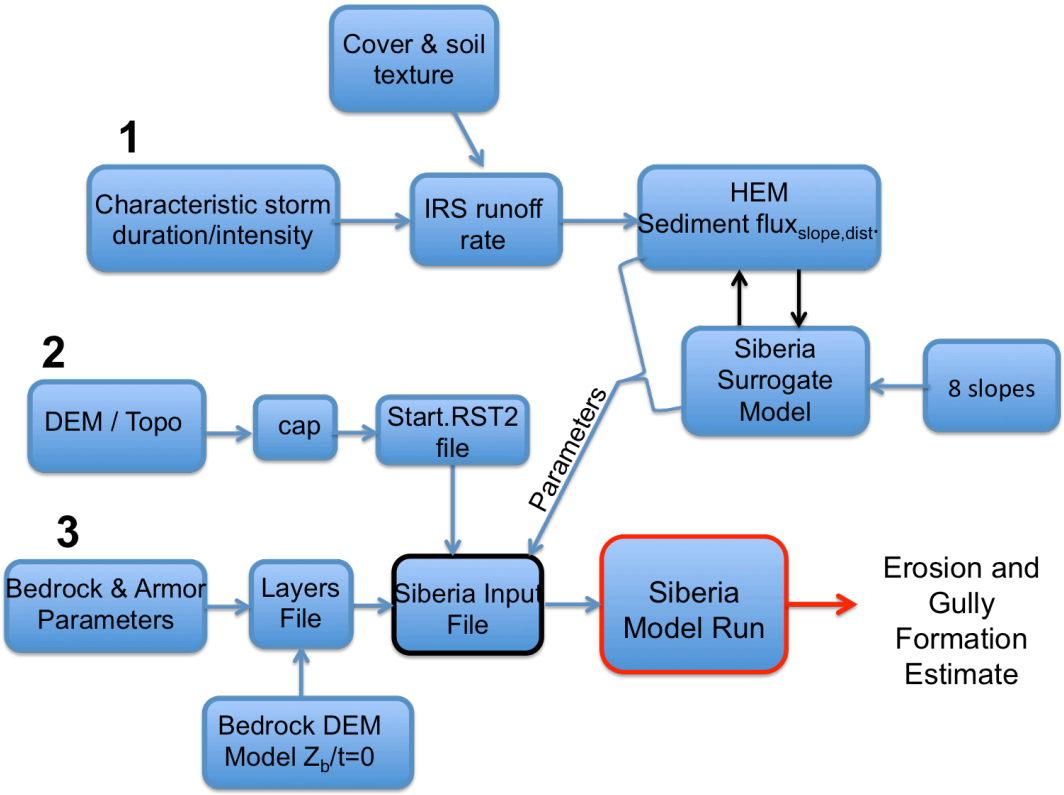

Figure 2-2. MDA G erosion model framework

Values for the parameters *B*, m, and *n* in SIBERIA were developed using the Infiltration and Runoff Simulation (IRS) model, version 9 (Stone et al., 1992), and the HEM sediment transport model (Lane et al., 2001). To predict runoff depth from a slope for a given storm, the IRS model is parameterized with information including soil texture class (e.g., loam and sandy loam), and canopy and ground cover. The runoff is then used as input for HEM, which also includes percent cover and soil information to estimate sediment production along a set of terrain profiles. Finally, SIBERIA parameters *B*, *m*, and *n* are calibrated using sediment flux output from eight simulated HEM slopes as a calibration target (Figure 2-3).

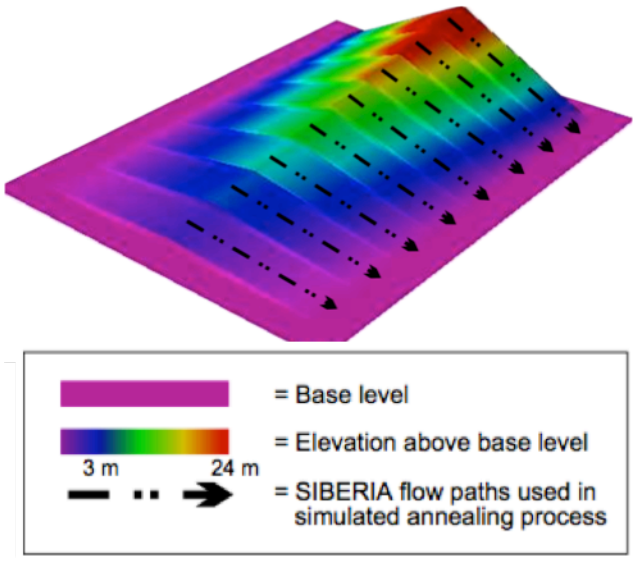

Figure 2-3. SIBERIA calibration to 8 HEM slopes

The timing and intensity of the precipitation falling on the disposal site plays an important role in determining the rates and patterns of erosion at MDA G. SIBERIA applies an average annual rainfall event and the geomorphically effective runoff event when simulating landscape evolution. This modeling approach requires the definition of a rainfall event and resulting runoff event which, when applied annually to the site, projects sediment yields that are assumed to be similar to those associated with a series of storms that vary in intensity and duration.

A storm with a 2.33-year return period is frequently taken to represent a mean annual event, since this is the corresponding recurrence period for early flood frequency modeling based on the Gumbel statistical distribution (Dalrymple, 1960; Sveinsson et al., 2001). To constrain erosion rate uncertainty, the SIBERIA modeling conducted in 2005 and 2010 adopted rainfall events for MDA G with return periods of 2 and 5 years (Wilson et al., 2005); these return periods bracket the 2.33-year storm generated from the National Oceanic and Atmospheric Administration (NOAA) Atlas 14 (Bonnin et al., 2006) for the semiarid southwest. The use of these return periods was further supported by data collected over approximately 16 years from an analog rangeland site at the Santa Rita Experimental Range in Arizona (Lane, 2003), where 16-year average sediment yields were similar to those observed for storms having a return period between 2 and 5 years

(Wilson et al., 2005, Table 1).

The NOAA Atlas 14 (Bonnin et al., 2006) was also used to parameterize the characteristic storm used to estimate runoff in IRS. The characteristic storm was 6 hours long with 29.5 mm total rainfall. IRS represents a variation of rainfall intensity over the duration of the storm, with the peak set in the middle of the 6-hour period and a ratio of peak rainfall intensity to average intensity set at 17.1, meaning that for a brief period the rainfall intensity was 1.4 mm/min.

The canopy and ground cover characteristics simulated in IRS were used to distinguish between the low-, moderate-, and high-erosion scenarios. They were defined, in part, using information collected from the17 hillslope profiles shown in Figure 2-4. Field measurements conducted along these profiles quantified hillslope length and slope, and canopy and ground cover fractions (Table 2-1).

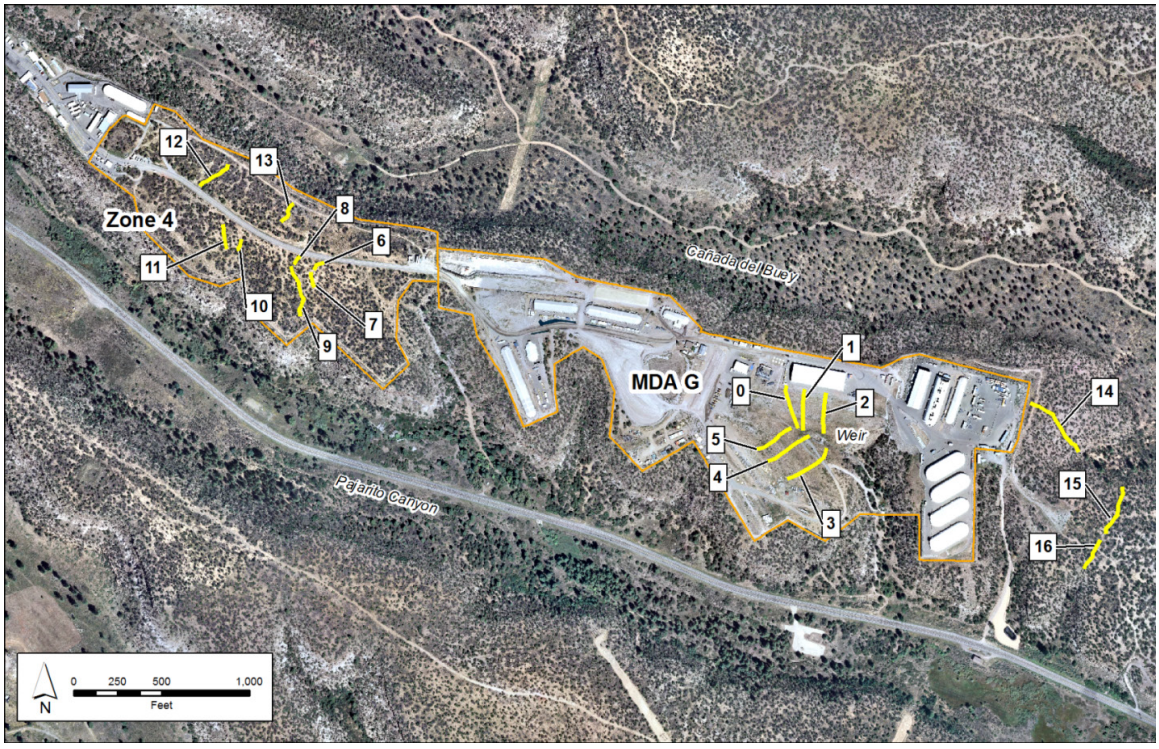

Figure 2-4. Locations of hillslope profiles

Table 2-1. Hillslope Profile Characteristics

Profile No.	Profile Name	Total Slope Length (m)	Segments		Average Cover (%)	
			Number	Averag e Slope	Canopy	Ground
0	Area G-1	78	10	11.2	61	23
1	Area G-2	74	5	11.9	64	24
2	Area G-3	72	6	13.0	63	22
3	Area G-4	91.5	10	8.2	20	33
4	Area G-5	85.5	10	10.0	24	46
5	Area G-6	72.4	11	10.6	26	41
6	EX-1N	30.5	4	5.0	8	27
7	EX-1S	27	4	4.1	2.9	7.9
8	EX-2N	18.3	4	9.1	15	44
9	EX-3S	113.5	15	5.5	26	40
10	EX-4S	22	4	6.2	12	32
11	EX-5S	43.5	5	6.4	6.9	17
12	EX-6N	66.5	6	6.2	32	61
13	EX-7N	40	7	10.5	27	57
14	East-1E	138	10	12.2	29	72
15	East-2N	94.5	9	11.0	29	69
16	East-2S	74	7	7.4	18	54

[a] *Segment slopes were weighted by the horizontal length of each segment to calculate the average profile slope; horizontal lengths were calculated using the slope angle and segment length.*

Canopy cover includes anything that may intercept a raindrop before it hits the ground surface, including branches, leaves, stems, and other obstructions. Ground cover was recorded if the soil surface was covered by rock, plant litter, plant basal stem, or other objects that shield the soil or obstruct flow along the profile. Each profile was divided into at least four segments based on changes in slope and ground cover, with each segment sampled uniformly at least 20 times (See Crowell, 2013, Table 2-2).

Eleven of the 17 hillslope profiles occur outside of MDA G and are similar insofar as they are located in relatively undisturbed piñon-juniper woodland. Figure 2-5 shows a typical profile immediately to the west of MDA G that begins near the trunk of a piñon or

juniper atop a raised mound and extends over mostly open ground until channelization is observed. Ground cover generally consists of plant litter, gravel or small rocks, basal stems of forbs and grasses, and biological soil curst pedicles. The 11 hillslope profiles located in and around MDA G provide representative low, medium, and high vegetation cover, and include profiles that have been irrigated to reestablish vegetation following disposal disturbance (Figure 2-6).

Figure 2-5. View of the base of profile 10, typical segment of a profile from west of MDA G.

Figure 2-6. Profile 2 spans covered pits planted with irrigated forms

Soil properties also play a significant role in determining erosion potential. The IRS and HEM modeling conducted to generate reference fluxes for parameterizing SIBERIA initially used sandy loam characteristics. The particle size distribution of this material is analogous to that of crushed tuff (Springer, 2004), which is the standard material used at MDA G for fill, daily cover of waste, and operational closure caps. The dominant soil unit mapped atop mesas of the Pajarito Plateau is the Hackroy Sandy Loam. Additionally, the engineered cover design adopted for the PA/CA includes a 6 percent clay admixture to increase strength and decrease infiltration while minimizing compaction (Day et al., 2005). An additional suite of IRS and HEM simulations was performed using characteristics of a loam soil to include the effects of the additional clay content. HEM assigns an erodibility factor of 2.31 to a sandy loam, and 1.84 to a loam (Lane et al., 2001).

Rainfall-runoff simulations were conducted with the IRS model for the 17 hillslope profiles using the rainfall event return periods and soil properties discussed above. The results of the modeling, updated in 2010, are summarized in Table 2-2. The lowest projected runoff is associated with the 2-year storm and a sandy loam soil, and the highest with the 5-year storm and a loam soil. The runoff projections for loam were generally greater than those estimated for sandy loam; runoff was greatest for the 5-year return period regardless of soil type.

Table 2-2. Runoff Projections for the Hillslope Profiles

Profile		Average Cover (%)		Estimated Runoff from 6-hr Storm (mm / storm)			
				2-yr Return Period		5-yr Return Period	
No	Name	Canopy	Ground	Sandy Loam	Loam	Sandy Loam	Loam
0	Area G-1	61	23	1.1	5	4.8	10.2
1	Area G-2	64	24	0.8	4.7	4.3	9.7
2	Area G-3	63	22	1	5	4.6	10
3	Area G-4	20	33	3.4	7.6	8.3	14
4	Area G-5	24	46	2.2	6.4	6.8	12.3
5	Area G-6	26	41	2.4	6.6	7	12.6
6	EX-1N	8	27	5	9.3	10.1	15.7
7	EX-1S	2.9	7.9	6.7	11.1	12.8	17.5
8	EX-2N	15	44	3	7.2	7.9	13.5
9	EX-3S	26	40	2.4	6.7	7.1	12.7
10	EX-4S	12	32	4.3	8.5	9.2	14.9
11	EX-5S	6.9	17	5.8	10.1	11.4	16.5
12	EX-6N	32	61	0.82	4.7	4.3	9.7
13	EX-7N	27	57	1.4	5.4	5.4	10.8
14	East-1E	29	72	0.46	4.2	3.6	9.1
15	East-2N	29	69	0.58	4.4	3.8	9.3
16	East-2S	18	54	2.2	6.4	6.7	12.2
Mean		27	39	2.6	6.7	7	12.4
Standard Deviation		19	19	1.9	2.1	2.7	2.6

The low-, moderate-, and high-erosion scenarios were assigned on the basis of the results shown

The runoff projections as a function of canopy and ground cover developed using the IRS model are discussed in Crowell, 2013, Figures 2-5, and 2-6). The IRS simulations show that runoff decreases when ground cover or canopy cover increases. Ground cover works to slow runoff by disrupting overland flow, whereas canopy cover provides additional storage for incoming precipitation. Reducing flow from increased ground and canopy cover fractions tends to promote increased infiltration.

Soon after site closure, ground cover fraction close to 100 percent may develop because of the initial fertilizer and soil amendments to be applied in order to establish forbs and grasses (Day et al., 2005). However, it is expected that over time the site will transition from grassland to woodland where canopy and ground cover fractions are expected to resemble conditions reported in Table 2-3.

The low-, moderate-, and high-erosion scenarios were assigned on the basis of the results shown in Table 2-2; the characteristics of the three scenarios are summarized as input in to IRS and HEM in Table 2-3. The low erosion scenario was defined as one in which the final cover consists of sandy loam, supports a healthy plant community, and is subject to the less severe 2-year rainfall event. The moderate-erosion scenario assumes a cover of sandy loam, less canopy cover, and a 5-year rainfall event. The runoff predicted for this configuration slightly exceeds that estimated for a loam cover subject to a 2-year storm. The high-erosion scenario assumes poor plant cover, a loam soil characterized by increased runoff, and the more severe rainfall event. The corresponding calibrated SIBERIA parameters fitted to the eight simulated HEM slopes depicted in Figure 2-3 for the low- moderate- and high-erosion rates are shown Table 2-3.

Table 2-3. Characteristics of Erosion Scenarios Implemented in IRS and HEM, and the Corresponding Calibrated SIBERIA Input Parameters for the Low- Moderate- and High- Erosion Scenarios

Model Parameters	Low	Moderate	High
Hillslope Erosion Parameters for IRS & HEM			
Soil Texture	Sandy Loam	Sandy Loam	Loam
Canopy Cover / Ground Cover (%)	70 / 70	30 / 70	30 /30
Landscape-Forming Return Interval [yr]	2	5	5
Excess Runoff [mm]	2.6	7	1.2
SIBERIA Model Parameters			
B = Grid Cell Runoff-driven Erosion [-]	9.4e-6	4.2e-5	6.8e-4
M = Area Sediment Yield Parameter [-]	1.6	1.6	1.3
N = Slope Sediment Yield Parameter [-]	0.86	0.87	0.86
D_z = Diffusion Coefficient [kg/m]	0.003	0.0025	0.005

2.2.2 Initial Domain Landform

Following Branch 2 in the model workflow illustrated in Figure 2-2, a DEM for MDA G that includes the engineered final cover shape is used to assign the initial landform shape and elevation (Figure 2-7). Figure 2-8 shows the approximate thickness of non-native material (both cover and additional fill above bedrock outside the pit areas) that is expected to be present above the bedrock surface following construction of the final cover. The estimated thickness of non-native material does not account for clean fill emplaced in the waste pits. The engineered cover will provide a minimum of 2-3 m cover depth over filled waste pits and shafts, while portions of the axis of the final cover may attain thicknesses of 10 m above bedrock, and additional fill is placed in the main, southeast side canyon (Figure 2-8). The final cover will be engineered to limit plant and animal intrusion into waste and to reduce infiltration of water into the waste to minimize radionuclide transport to

the regional aquifer. The reduction of infiltration will increase surface runoff, and therefore increase the erosive force to form gullies in the engineered final cover.

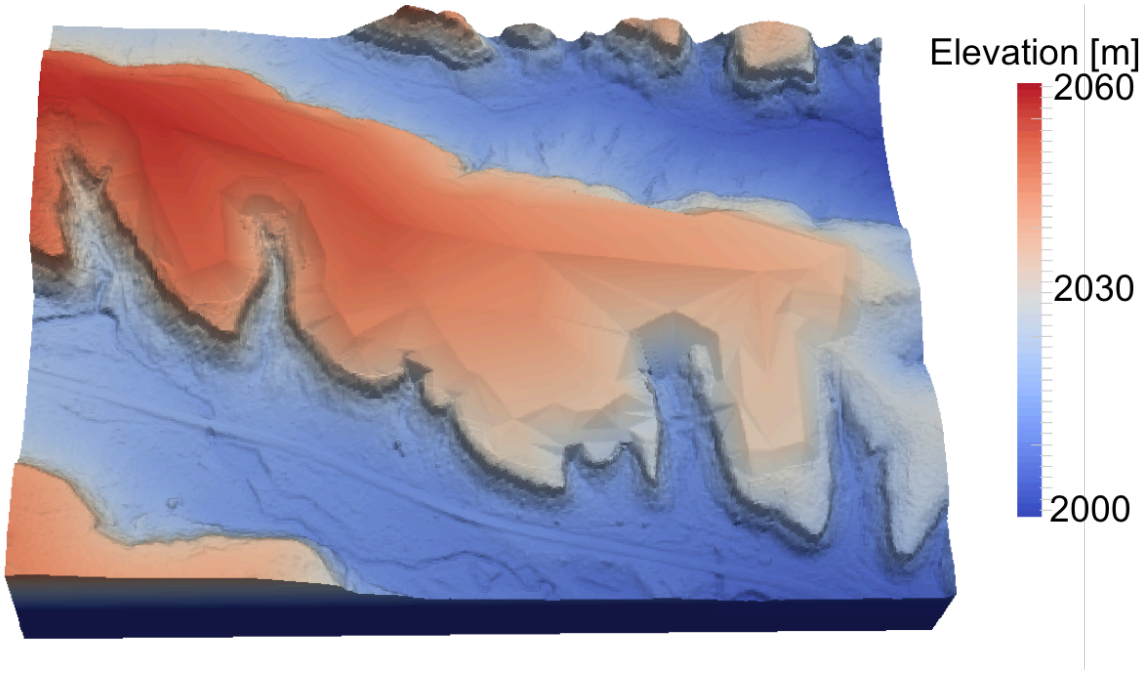

Figure 2-7. Initial domain shape and elevation (m) of the MDA G final cover and surrounding topography

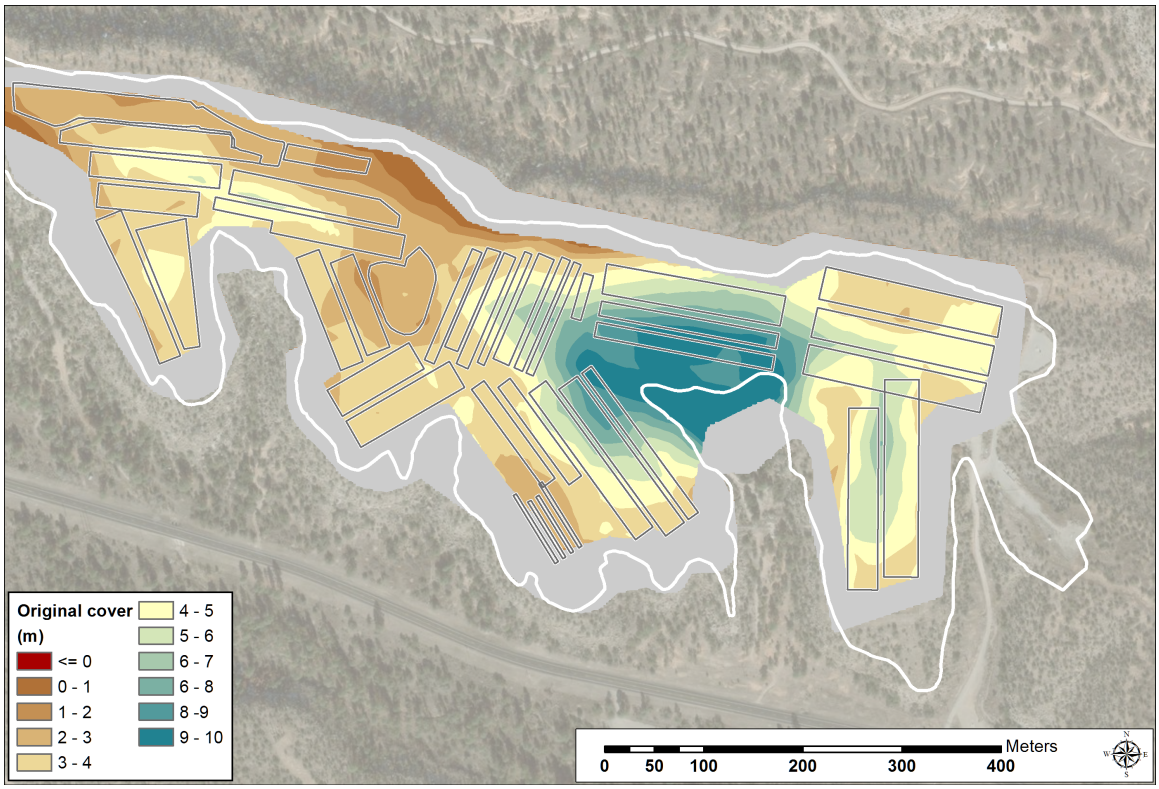

Figure 2-8. Initial (after closure) estimated thickness (m) of non-native material above bedrock. The thickness accounts for the engineered cover and fill outside of pits but within the riprap armor. Clean fill within pits is not included in the estimated thickness.

Using the updated version of SIBERIA (8.33), a bedrock layer is now included in the model domain shown in the workflow steps outlined in Branch 3 (Figure 2-2). The top of the bedrock layer is designated by an estimated bedrock surface (Figure 2-9), and its thickness is represented as an approximately 100-meter layer down to an elevation of 1900 m. Waste pits are etched into the bedrock to the pit basement (bottom) elevation for the SIBERIA calculations (Figure 2-9). A ring of riprap armoring that is 0.6 meters in depth and variable width, as shown in Figure 2-10, is placed around the mesa to prevent excessive head cutting from initiating along the mesa edge. The bedrock and armor are assigned the same reduced erodibility properties by setting *B* two orders of magnitude lower than is used for the final cover material.

Figure 2-9. Bedrock elevation with waste pits etched in, used for SIBERIA calculations.

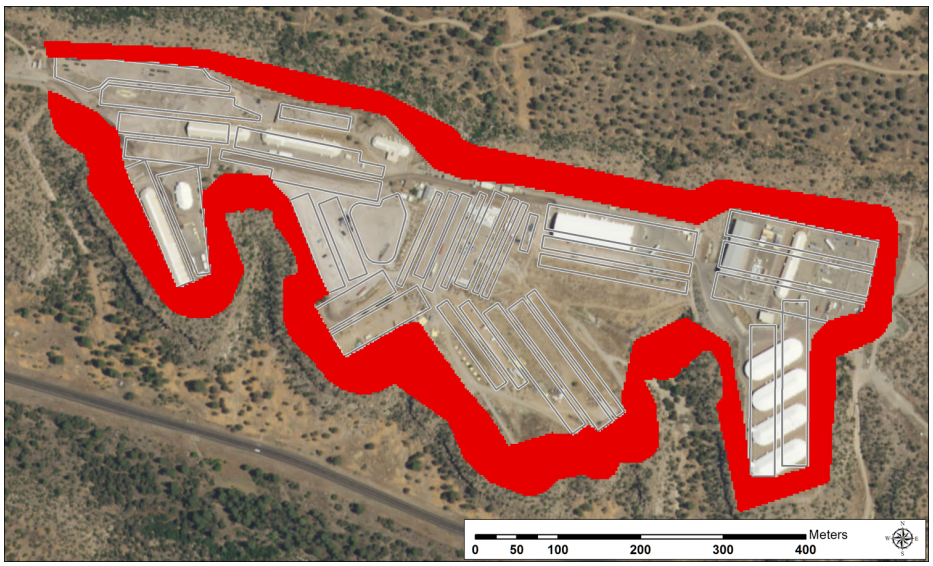

Figure 2-10. Riprap armor (red) placed around the MDA G waste repository site.

2.2.3 Model Simulations

The SIBERIA modeling conducted in 2005 (Wilson et al., 2005), in 2008 (LANL, 2008), and in 2010 (French and Crowell, 2010) projects 1,000 year erosion rates for the low-, moderate-, and high-erosion scenarios. The purpose of the current analysis is to evaluate erosion to 10,000 years at MDA G for the low-, moderate- and high-erosion scenarios using the parameters listed in Table 2-3.

An additional model update was used that implements the Dinfinity flow direction algorithm (Tarboton 1997; Wilgoose, 2005). The Dinfinity algorithm calculates the steepest down-slope direction and directs sediment flow based on 8 triangular facets in a 3x3 cell window. Sediment flow is then partitioned to a maximum of two neighboring cells based on the flow direction calculation. In contrast, the original formulation used a D8 formulation where flow is directed into only one of the eight adjacent cells. By switching to the Dinfinity algorithm, sediment flow more precisely follows the terrain, resulting in 1) increased convergent flow, which affects channel erosion, and 2) gradually changing flow runoff and sediment flux direction at a given location over time. Figure 2-11 shows the erosion channels that result from the SIBERIA calculation using the original D8 flow direction algorithm and those that result using the Dinfinity algorithm. The D8 flow algorithm leads to linear channel formation, whereas, the Dinfinity formulation leads to more natural, feathered and varied channel formation.

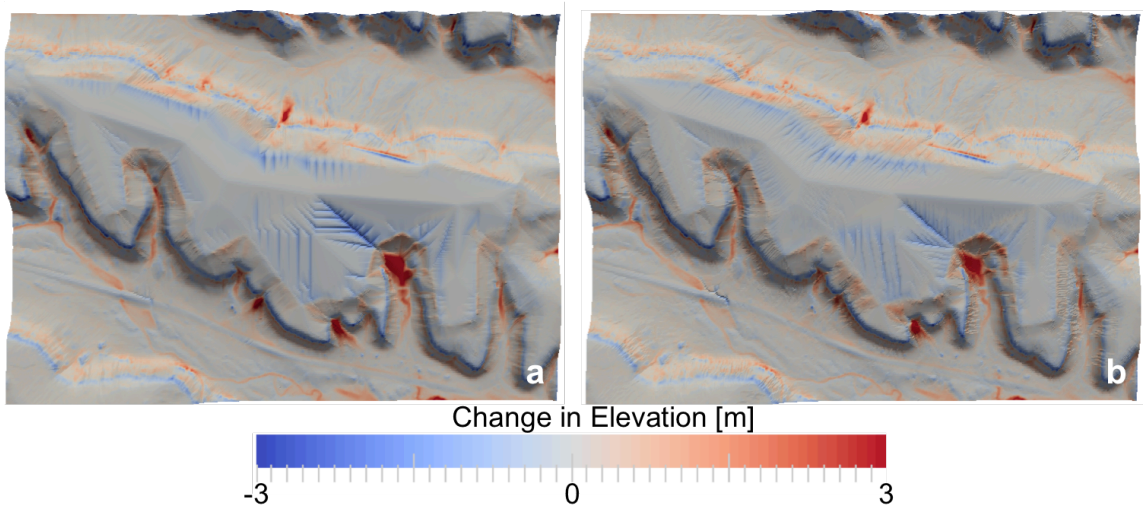

Figure 2-11. Erosion channels simulated (a) using the D8 flow direction algorithm, and (b) using the Dinfinity flow direction algorithm.

3.0 Results

This section summarizes results of the extended 10,000-year erosion forecasts in comparison to the 1,000-year forecasts. The comparisons between the compliance period forecasts (1,000 year) and the extended forecasts (10,000 year) are presented in Section 3.1 as well as the erosion forecast uncertainty. Section 3.2 illustrates the long-term effect of the riprap armor. Section 3.3 presents results for simulated sediment deposition around the mesa at MDA G, and a discussion of the implications of the predictions.

3.1 10,000-Year Erosion Analysis

As expected, substantially more erosion is observed over the 10,000-year simulations than for the 1,000-year simulations (Figure 3-1). Both the 10,000-year moderate- and high-erosion scenarios have localized areas with approximately 10 meters maximum loss of elevation on the mesa. Interestingly, the long-term low-, moderate-, and high- erosion scenarios express vastly different landscape evolution. The long-term, high-erosion scenario, which uses the highest diffusion coefficient (D_z) (Table 2-3), results in a general smoothing of the landform and a loss of cover material by erosion over large swaths on the mesa. Non-intuitively, the moderate-erosion scenario shows the deepest gully formation, with only a moderate overall lowering of the landscape elevation. The moderate-erosion scenario also has the lowest D_z (Table 2-3) and thus has limited diffuse erosion across the landscape. The low D_z when combined with moderate B parameter value (Table 2-3) exacerbates gully formation. The low-erosion scenario with low B and D_z (Table 2-3) has the lowest long-term erosion and minimal gully formation.

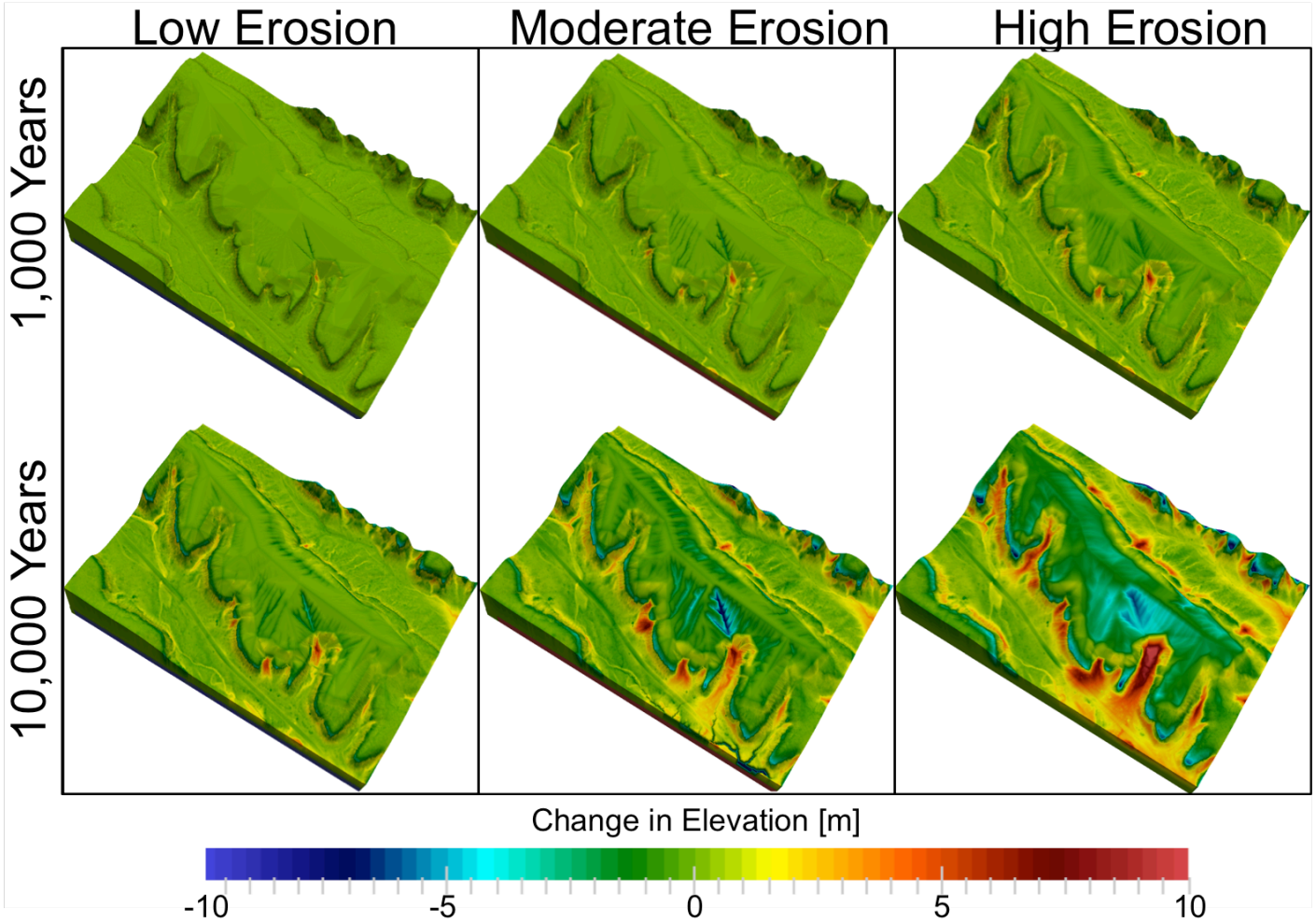

Figure 3-1. Change in elevation (m) maps for low-, moderate-, and high-erosion cases. The top row shows results for the 1,000-year compliance period. The bottom row shows results at 10,000 years, 9,000 years beyond the compliance period.

The changes in elevation from the original surface elevation after 10,000 years for the low- and high-erosion cases are shown in Figure 3-2. These figures illustrate the loss of cover and fill material from the mesa and deposition of material into the neighboring side canyons. The low-erosion scenario indicates that only a few waste pits, located in the south central portion of MDA G, will lose up to 1.5 meters of cover material, while little (< 0.5 m) to no loss occurs over much of the site after 10,000 years. One small gully of between 1.5 to 2.5 meters in depth is projected to bisect a single pit (Figure 3-2). In contrast, the high-erosion scenario shows that much of the site will lose between 1.5 to 2.5 meters of cover material, with some of the south central portion of MDA G losing between 2.5 to 5 meters of the cover material (Figure 3-2), but virtually zero bedrock material is eroded. Additionally, the high-erosion case projects that localized areas near the large southeastern side canyon that cuts into Mesita del Buey, may experience greater than 5 meters of cover and fill loss. However, it should also be noted that the locations with the highest erosion are either near the crest of the final cover or co-located with a large gully with planned fill, both locations having cover material that is approximately 10 meters deep.

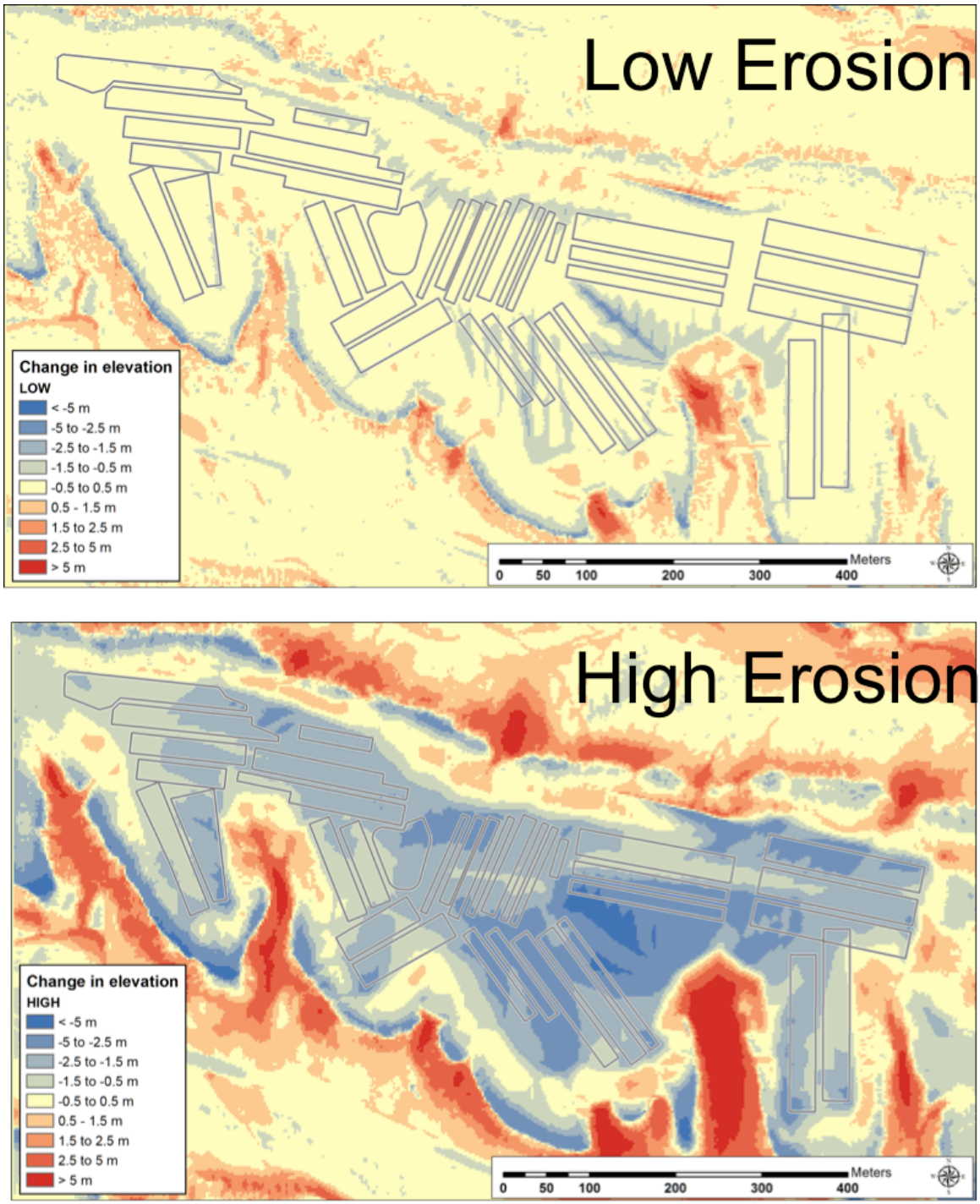

Figure 3-2. Change in surface elevation (m) after 10,000 years of erosion with pit locations shown for the low-erosion (top) and high-erosion (bottom) cases.

Figure 3-3 shows the resultant changes in "cover thickness above bedrock" for these same two scenarios. As explained previously, this thickness is estimated and includes the non-native material above bedrock (i.e., the engineered cover and clean fill outside the pit areas) within the riprap armor. To estimate the remaining thickness, the elevation of the bedrock used in SIBERIA was subtracted from the simulated cover elevation. To estimate the original bedrock surface across pit locations, the locations were filled by interpolating the elevations around the pits using a triangulated network of known points. Because both the initial thickness of the material above bedrock (Figure 2-8) and the changes in elevation due to erosion (Figure 3-2) are highly variable, the estimated thickness of material above bedrock remaining at 10,000 years is used to illustrate areas where losses may approach the level of the waste pits. For the low erosion scenario (Figure 3-3, top) and in areas with pits present, there is a minimum of 1-2 m of cover/fill above bedrock remaining after 10,000 years. For the high-erosion scenario, there are a few places where the cover/fill material is predicted to erode down to the level of the bedrock and complete loss of the overlying cover/fill material will occur. Of the few locations that erode down to bedrock in the high-erosion scenario above the pits, very little, if any, erosion occurs past the bedrock, and the surface remains above the top of waste at 10,000 years as sufficient clean fill below the estimated bedrock grade but above the waste is present. We note that these results are quite uncertain, and the thickness of material above bedrock is estimated, but the simulations provide a general sense of erosion patterns and soil loss across the site.

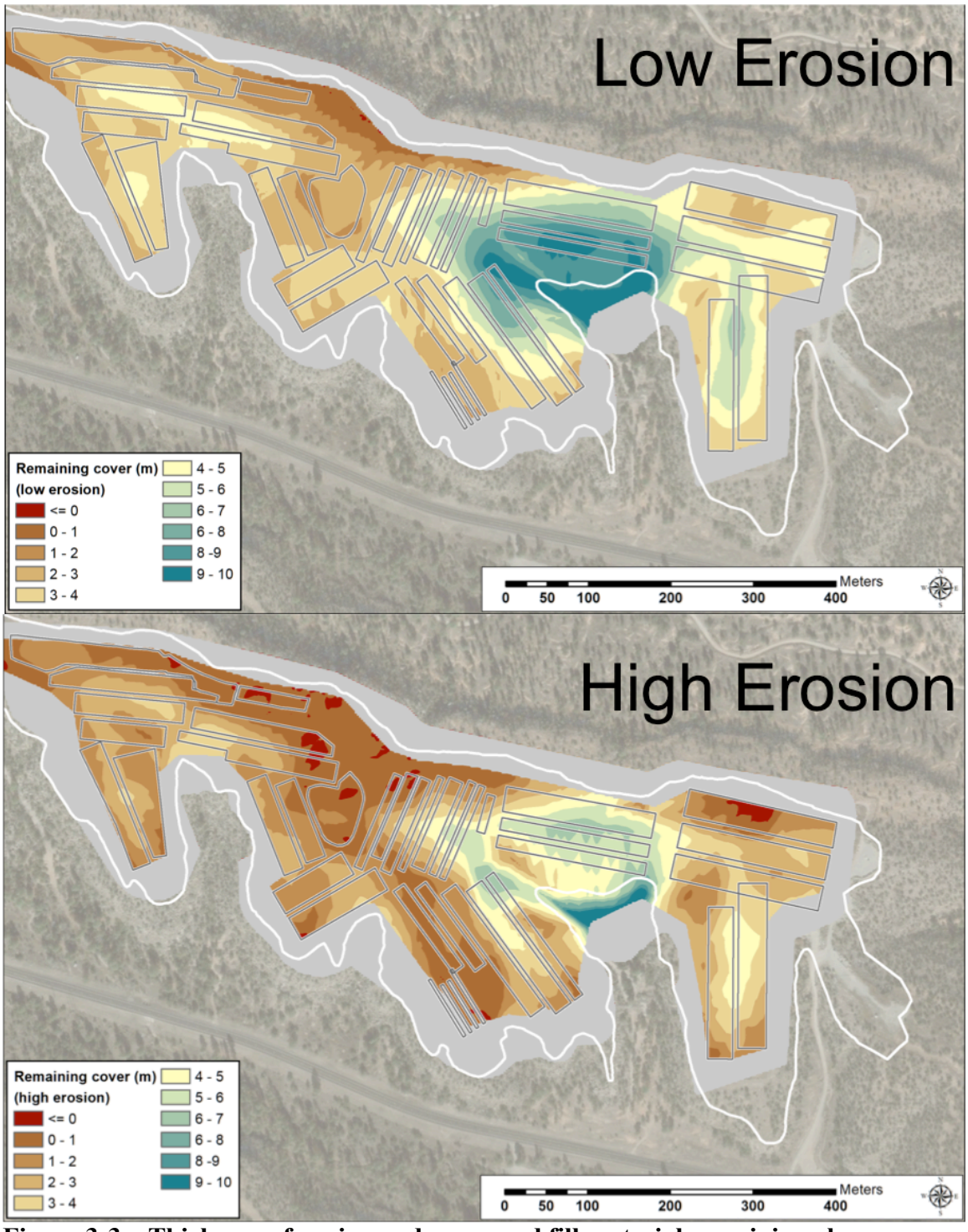

Figure 3-3. Thickness of engineered cover and fill material remaining above bedrock after 10,000 year simulation period, clipped by the riprap armor layer around the mesa top for the (top) low-erosion and (bottom) high-erosion scenarios.

3.2 Impact of Riprap Armor

Despite the large amount of erosion for both the moderate- and high-erosion scenarios, no erosion is predicted to occur around the mesa edges (Figure 3-4). This indicates the parameters used in the simulations for the riprap armor prevent erosion along the mesa edges, assuming the riprap will not degrade or fall from the mesa edge. Even though the moderate-erosion case predicts extensive gully formation in the engineered final cover, the mesa edges maintain their initial elevation, which indicates that the gullies do not result from upslope head cutting from the edges of the mesa. Rather, the gullies predicted under the moderate-erosion scenario result from the erosive properties of the cover material and the low D_z.

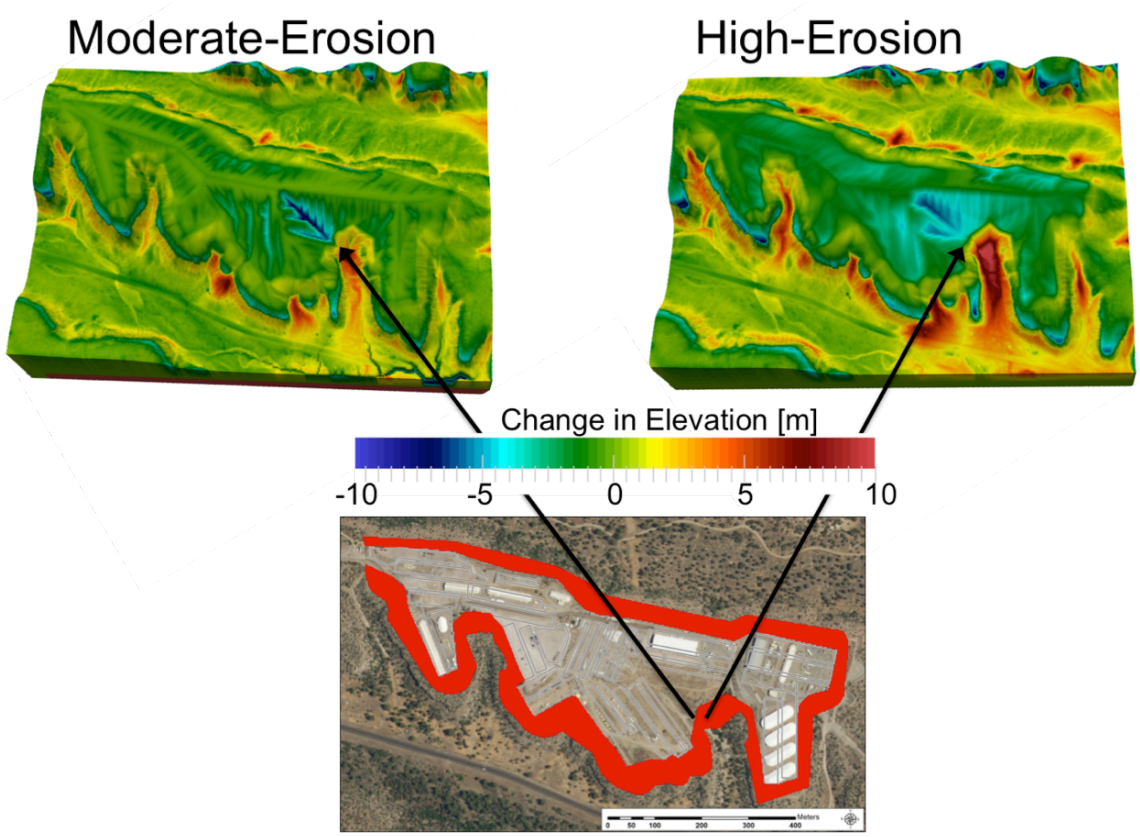

Figure 3-4. Placement of riprap armor is shown in the bottom figure; changes in surface elevation (m) for the moderate- and high-erosion scenarios are shown in the top two figures. The model predicts a ring of unchanged elevation where the riprap is present around the mesa edge.

3.3 Canyon Deposition

Both the moderate- and high-erosion scenarios predict areas of high sediment deposition, 10 meters or more after 10,000 years, in the canyon bottoms **(**Figure 3-5). The high-erosion scenario, in particular, shows extensive deposition, an indication of the large amount of sediment moved from the mesa top into the canyon bottoms. However, canyon filling is currently not the natural form observed on the Pajarito Plateau, and it is unlikely for the canyon bottoms to fill with 10 meters of sediment. The moderate-erosion scenario also shows considerable deposition in the canyon bottom although the prediction is more consistent with current geomorphology observed on the Pajarito Plateau. As part of the model validation process, simulated deposition in the canyon bottoms was evaluated against observed geomorphology of the plateau. In cases where canyons were filled with sediment, D_z was decreased to reduce diffusive properties of sediment deposition (Wilson, 2005). Given that the moderate-erosion scenario has the lowest D_z (Table 2-3) of the three scenarios tested, it would suggest that lowering D_z may result in more realistic erosion and landform projections, but may also reduce the sediment discharge needed to calibrate to SIBERIA to the observed hillslope transects (Figure 2-4). Alternatively, adjusting the m and n parameters to increase advection-driven transport may also reduce sediment deposition within canyon bottom channels. However, a possible culprit of the excessive canyon bottom deposition is the lack of simulated discrete events, such as large rainfalls, that would normally clear sediment from the canyon bottom. Another possibility is that an adjustment of n, the slope sediment yield parameter, may be required for the canyon bottoms.

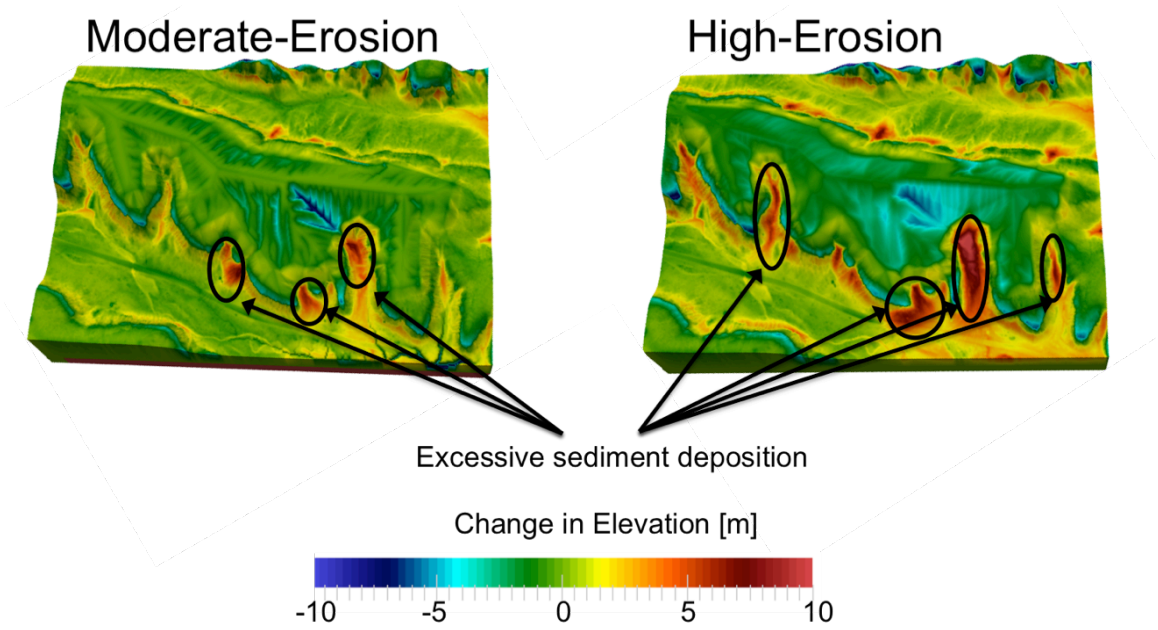

Figure 3-5. Locations of high sediment deposition

4.0 Discussion

The low-, moderate-, and high-erosion scenarios used to analyze the impacts of erosion over the 1,000-year compliance period are extended to a 10,000-year analysis. This analysis provides a valuable perspective of the long-term model behavior of SIBERIA and of the conceptual model design. Furthermore, it allows the evaluation of the development of site characteristics beyond the 1,000-year compliance period. However, results regarding the depths of erosion should be viewed as uncertain.

4.1 10,000-Year Forecast Uncertainty

Comparing the results between the low-, moderate-, and high-erosion scenarios after 10,000 years shows a great deal of uncertainty. Not only does the uncertainty span a wide range of total sediment movement off the mesa, but also the resulting land forms in the canyons and on the mesa top are different for each scenario. The high-erosion scenario produces rounded mesa tops and partially-filled canyon bottoms, whereas the moderate-erosion case produces incised gullies and sharp

mesa rims. In contrast to both the moderate- and high-erosion cases, the low-erosion case results in relatively little erosion.

Parameter uncertainty introduced during model parameterization accrues over the simulation to produce significantly different erosion forecasts. The initial parameter uncertainty between the low-, moderate-, and high-erosion scenarios is largely unavoidable as precise parameter values are unavailable. While SIBERIA can be parameterized directly using long-term rainfall, runoff, and sediment yield data, direct erosion measurements are not available for MDA G. This is primarily because the final cover is not in place to study how erosional forces will reshape the cover over time. Therefore, surrogate sites and a reduced-order model were used to provide estimates for parameters used in SIBERIA. Although extensive model validation was performed (Wilson et al., 2005), there is substantial initial parameter uncertainty. Moreover, while this initial parameter uncertainty may appear small (Table 2-3), over the course of 10,000-year simulations, the differing parameters large ranges in possible sediment yields and landscape evolution.

In addition to parameter uncertainty, calibrating SIBERIA to a reduced-order model may result in model inconsistencies over long time scales. The reduced-order model is incapable of resolving the 3D erosion physics necessary to characterize diffusive processes relative to advective erosional processes. The low-, moderate-, and high-erosion scenarios were determined based on the IRS and HEM models, which simulate erosion only on 1D flow paths with uniform slopes. In contrast, SIBERIA simulates erosion across a 3D landscape and represents diffusion-dominated and transport-dominated erosion and deposition processes (Figure 2-2) via a relationship between *m* and *n*, which determine the area sediment yield and the slope sediment yield, respectively. In order to parameterize SIBERIA for low-, moderate-, and high-erosion scenarios, the *m* and *n* parameters were calibrated to HEM results that again cannot simulate erosional differences between diffusion-dominated and transport-dominated mechanisms. Therefore, while the *m* and *n* parameters may provide the best model fit to a short time 1D calibration, they may

not remain applicable for longer 3D representations where, over longer time, more channels may form, or alternatively some channels may aggregate through diffusional process such as slope creep and sediment deposition.

4.2 Geomorphically Effective Runoff Event Assumption

As stated in Section 2.1.2, SIBERIA relies on the "geomorphically effective runoff event" assumption, which is computationally efficient and key for simulating long-time scales because it assumes average, steady-state, behavior. However, the assumption may also significantly bias both the 1,000- and 10,000-year erosion assessments, and may result in under estimates of total erosion (Coulthard et al., 2013). Furthermore, the excessive canyon sediment deposition shown in Figure 3-5, which spans low and high gully formation characteristics, suggests that discrete events are needed to maintain the sharp canyon and mesa formation characteristic of the Pajarito Plateau. Likewise, if the model is unable to represent discrete erosion events that tend to clear canyon bottoms from sediment buildup, it is conceivable that discrete erosion events could affect the mesa tops by excluding more energetic events that might lead to, for example, enhanced gully formation.

Additional model bias may be introduced by insufficiently identifying the variability of rainfall and runoff over the simulation time period. Recently, a growing body of literature suggests that erosion and advection-driven transport rates of sediment tend to increase when discharge (runoff) variability increases (i.e. Tucker and Handcock, 2010; Molnar et al., 2006; Lague et al., 2005). The results of the SIBERIA calculations may not properly represent the effect of runoff variability in two ways: first, by not explicitly representing runoff variability, and second, by not parameterizing SIBERIA with long-term data that capture the runoff variability seen in the Southwest. Runoff and erosion data collected over a 16-year period from the Santa Rita Experimental Range analog rangeland site in Arizona (Lane, 2003) were used to support the choice of a 2.33 year storm return period for the simulated mean annual event by providing a bounding range of 2-5 years. It is unlikely that a 16-year

analysis captures the rainfall and runoff variability encountered over a 10,000- or even a 1,000-year period. Indeed, there is strong evidence for many multi-decadal droughts and wet periods in the past four hundred years (e.g. Swetnam and Betancourt, 1998; Sheppard et al., 2002), which may surpass the 2- and 5-year return periods used by French and Crowell (2010). Furthermore, the 2.33-year storm return period generated from the NOAA Atlas 14 (Bonnin et al., 2006) is based on historical data of 100 years and does not account for climate change. Climate change may introduce additional extreme responses from strengthened convective storm regimes (Del Genio et al., 2007) with fewer, but stronger, precipitation events (Trenberth et al., 2003) that may dominate runoff events on the Pajarito Plateau.

5.0 Conclusions and Potential Future work

5.1 Conclusion

A 10,000-year erosion forecast was performed using the current MDA G erosion modeling framework. Previous erosion modeling analysis was carried out through the 1,000-year compliance period following passive institutional control period. However, it is acknowledged that radioactive material may interact with the surrounding environment well beyond 1,000 years. Therefore, an extended erosion analysis was conducted to provide a long-term assessment of how erosion forces may continue to shape the surface at MDA G. In addition to extending the erosion analysis to 10,000 years, the model was improved by applying the Dinfinity algorithm to simulate channel migration and refined channel networks. The modeling framework was also streamlined and is now managed by the Model Analysis Toolkit (MATK) wrapper function. The use of MATK also enables efficient calibration and sensitivity analysis executing parallel computation of SIBERIA ensemble members.

As expected the 10,000 year erosion simulation show considerably more erosion then the 1,000 compliance period analysis. However, all three (low-, moderate-, and high-erosion scenarios) 10,000 year SIBERIA simulations show that much of the

MDA G site will have remaining cover, with only a few small areas that have eroded down to the original bedrock for the high-erosion scenario. It should be also noted that of the small areas that are predicted to erode down to bedrock, little if any additional erosion takes place below the bedrock grade. Furthermore, the armor ringing the mesa top is simulated to be rather robust and maintains a rim elevation for the simulation period that prevents excessively deep channelization into the mesa.

The three erosion scenarios (low, moderate, and high) simulated to 10,000 years also exposed a large range of simulation uncertainty resulting in very different long term landform evolution and sediment fluxes for each scenario. The high-erosion scenario produced rounded mesa tops and filled in canyons, whereas the moderate-erosion scenario produced extensive deep gully networks. This extended model analysis further serves to identify model performance and, specifically, points to how the MDA G erosion modeling framework can be improved. The model analysis identified three significant methods for the erosion predictions by: 1) reducing initial parameter uncertainty through ongoing surrogate site data collection, 2) exploring alternative reduced order models for SIBERIA calibration targets that account for 2D or 3D erosion physics of diffusion versus advection erosion processes, and 3) exploring alternative LEMs that do not rely on the geomorphically effective runoff event assumption that assumes, over long time scales, erosion can be represented as a steady process, and runoff is considered as a constant, low-magnitude process that shapes the landscape. The 10,000 year analysis also brings to bear a current perspective of LEM's and the role the rainfall and runoff variability plays in landscape formation. The outlined methods for improving the erosion analyses are designed to reduce uncertainty in model and landform evolution. However, it should be noted that, in some cases, steps to reduce model uncertainty may produce estimates of erosion greater than the three cases simulated here. Never-the-less, the reduced erodibility of the bedrock and riprap armor will still likely prevent substantial excavation below bedrock grade.

5.2 Future Work

5.2.1 Incorporation of Erosion Results into the PA/CA Model

The erosion study presented in this report is research and development conducted to support MDA G. The study yields estimated patterns and rates of soil loss for low-, medium-, and high-erosion scenarios. The updated results have not been incorporated into the current PA/CA site model to determine the impact of these extended erosion scenarios on exposure or dose. Within the PA/CA GoldSim model, previous SIBERIA results are used to project rates of soil loss through time across several disposal regions at MDA G; these losses are used to update the thickness of the surface soil, cap, and waste layers through time for each region. In addition, previous SIBERIA results are used in the PA/CA model to assign sediment loads that are transported by erosion into different catchments in Cañada del Buey and Pajarito Canyon. The calculations assume that sediments that reach the mesa edge are transported to the canyon floors, where the deposition location of the sediment corresponds to the catchment directly below the point of departure at the mesa edge.

For the most part, erosion results in a gradual thinning of the cover over extended periods of time, and eroded sediments will be transported into the adjacent canyons. Over long time periods, erosion may make direct accessibility to the waste an exposure pathway. However, the main role of erosion in exposure is through the transport of contaminated sediment off into canyons. The sediment is assumed to be contaminated through time by biotic intrusion, in which disposed radionuclides are transported to the surface by plants whose roots penetrate into the waste and animals whose burrows extend into the waste. These radionuclides would then, in turn, be mixed with local sediment that is subject to offsite erosion. The resulting exposure pathways in the canyon results from exposure to contaminated soils, ingestion of contaminated soil, ingestion of food crops grown in contaminated soils, ingestion of animal products from animals raised on land having contaminated soil, and some airborne pathways.

Currently, the PA/CA model is set up to use SIBERIA results for the first 1,000 years after site close (i.e., no additional erosion occurs if the model is run for times longer than the 1,000-year compliance period). Incorporation of results from the 10,000-year erosion simulations presented here would allow for exposure and dose calculations through a 10,000-year uncertainty period.

5.2.2 Continued and updated validation

The large uncertainty demonstrated in the long-term assessment of the MDA G erosion model highlights the need to refine the model parameterization and validation. In order to create robust long-term erosion predictions, uncertainty in the model parameters must be reduced. A commendable attempt to provide the best estimate for SIBERIA parameters was initially performed using the data that were available at the time. However, the initial parameterization work concluded in 2005 (Wilson et al., 2005) and additional data have not been collected. In the past year, an attempt to locate and organize the original model validation data from all 17 slope profiles and from the Santa Rita Experimental Range site in Arizona, as well as from cover plots located in Technical Area 51 (Nyhan et al., 1997) was conducted. However, the original data could not be located and only the resulting publications are available (e.g., Lane et al., 1997; Reid et al., 1999). A continued effort to locate and organize the original data would be instrumental for helping refine model parameterization and reduce long-term erosion forecast uncertainty. If these data can be located, additional data since 2005, or in many cases starting before 2005, could augment the data archives to provide a longer record of observed erosion and runoff variability.

Disturbances, such as fire, are also known to greatly affect rainfall runoff relationships (Moody and Martin, 2001; Moody et al., 2013; Moody and Ebel, 2014) and could further introduce runoff and erosion rate variations (Cannon, 2001; Cawson et al., 2013; Hyde et al., 2014). Variance in runoff contributes to increased erosion rates. Often the culprit of increased runoff and sediment transport from fire

disturbance is the hydrophobic and hyperdry soil properties (Robichaud, 2000; Martin and Moody, 2001; Moody and Ebel, 2012), and physical soil crusting (Larsen et al., 2009), which are generally a function of fire severity (Keeley, 2009; Moody et al., 2016). Recently fire disturbances on the Pajarito Plateau have affected large areas causing increased erosion and runoff (Cannon and Reneau, 2000; Moody et al., 2008), undoubtedly high severity fire disturbance similar to the Cerro Grande Fire in 2000 and the Las Conchas Fire in 2011 will affect the Pajarito Plateau within the 1,000 year compliance period and 10,000 year erosion analysis. These types of disturbances that will have a direct effect on erosion rates should be considered when assessing long-term erosion rates and gully formation. Understanding how fire severity affects the infiltration properties of the engineered final cover at MDA G will help constrain the long-term variance of runoff and therefore could be used to augment the original calibration data.

Section 3.2 demonstrated the assumed effectiveness of the riprap armor around the mesa top. Assuming that the riprap lasts the entire 10,000 year simulation period, the gullies in the mesa top will not erode beyond a depth of the top of the riprap. However, this assumption may not hold given the precarious location of the riprap armor. Rock fall along the mesas edges on the Pajarito Plateau is a common occurrence (Miller et al., 2018), and the effect of a degraded riprap armoring needs to be assessed.

5.2.3 Alternative models

The extended 10,000 year analysis provides key insight into how SIBERIA simulates landscape evolution. More importantly, this exercise has identified two shortcomings in the MDA G modeling assessment that could be improved in future assessments: 1) better constrained erosion parameters and calibration methods that account for 3D physics, and 2) better resolution of discrete events rather than relying on the geomorphically effective runoff event assumption. Testing of model alternatives in both the calibration process and forward model simulations could

then be used to improve erosion projection fidelity. Rather than relying on 1D surrogate models that cannot resolve diffusion and advective erosion processes as calibration targets, 2D and 3D alternatives that capture both upslope and channel processes could be explored. In addition alternative LEM's could be evaluated such as CASCADE (Braun & Sambridge, 1997), CAESAR (Coulthard et al., 2000; 2005), and CHILD (Tucker & Bras, 2000). These newer LEMs represent variable runoff over time, and in some cases, spatially distributed runoff. While the new class of LEMs will be more computationally expensive, the additional computational expense is 1) not prohibitive on current LANL computational resources, and 2) likely to increase erosion forecast fidelity.

6.0 References

Bonnin, G.M., D. Martin B. Lin, T. Parzybok, M. Yekta, and D. Riley, 2006, NOAA Atlas 14: Precipitation-Frequency Atlas of the United States Volume 1 Version 4.0: Semiarid Southwest (Arizona, Southeast California, Nevada, New Mexico, Utah), National Weather Service, 261 pp.

Braun J, Sambridge M. 1997. Modelling landscape evolution on geological time scales: a new method based on irregular spatial discretization. Basin Research 9: 27–52.

Cannon, S. H. (2001), Debris-flow generation from recently burned watersheds, *Environmental & Engineering Geoscience*, *7*(4), 321-341. doi: 10.2113/gseegeosci.7.4.321.

Cannon, S. H., and S. L. Reneau (2000), Conditions for generation of fire-related debris flows, Capulin Canyon, New Mexico, *Earth Surface Processes and Landforms*, *25*(10), 1103-1121.

Cawson, J., G. Sheridan, H. Smith, and P. Lane (2013), Effects of fire severity and burn patchiness on hillslope-scale surface runoff, erosion and hydrologic connectivity in a prescribed burn, *Forest Ecology and Management*, *310*, 219-233. doi: 10.1016/j.foreco.2013.08.016.

Coulthard, T.J., Kirkby, M.J. and Macklin, M.G., 2000. Modelling geomorphic response to environmental change in an upland catchment. *Hydrological Processes*, *14*(11-12), pp. 2031-2045.

Coulthard, T.J., Lewin, J. and Macklin, M.G., 2005. Modelling differential catchment response to environmental change. *Geomorphology*, *69*(1-4), pp. 222-241.

Coulthard, T.J., Neal, J.C., Bates, P.D., Ramirez, J., Almeida, G.A. and Hancock, G.R., 2013. Integrating the LISFLOOD-FP 2D hydrodynamic model with the CAESAR model: implications for modelling landscape evolution. Earth Surface Processes and Landforms, *38*(15), pp. 1897-1906.

Crowell, K.J., 2013, Sensitivity of Surface Erosion Modeling For Los Alamos National Laboratory Technical Area 54, Area G, Los Alamos National Laboratory Report LA-UR-13-24013.

Dalrymple, T., 1960, Flood Frequency Analyses, Manual of Hydrology: Part 3. Flood-Flow Techniques, USGS Water Supply Paper 1543-A, 86 pp.

Day, M.S., C.K. Anderson, and C.D. Pedersen, 2005, Conceptual Design of the Earthen Cover for at Los Alamos National Laboratory Technical Area 54, Material Disposal Area G, URS Corporation Report to LANL, Los Alamos National Laboratory Report LA-UR-05-7394, September.

Del Genio, A. D., M. S. Yao, and J. Jonas (2007), Will moist convection be stronger in a warmer climate?, Geophysical Research Letters, *34*(16). doi: 10.1029/2007GL030525.

Department of Energy (DOE), 2001, Radioactive Waste Management, U.S. Department of Energy Order 435.1, (change 1 to document issued July 9, 1999), August 28.

French, S. and Crowell, K.J., 2010, Updated Surface Erosion Modeling for Repository Waste Cover at Los Alamos National Laboratory Technical Area 54, Area G, Los Alamos National Laboratory Report LA-UR-10-06442, September.

Hyde, K. D., A. C. Wilcox, K. Jencso, and S. Woods (2014), Effects of vegetation disturbance by fire on channel initiation thresholds, *Geomorphology*, *214*, 84-96. doi: 10.1016/j.geomorph.2014.03.013.

Keeley, J. E. (2009), Fire intensity, fire severity and burn severity: a brief review and suggested usage, *International Journal of Wildland Fire*, *18*(1), 116-126. doi: http://dx.doi.org/10.1071/WF07049.

Laflen, J., L. Lane, and G. Foster, 1991, "WEPP- A New Generation of Erosion Prediction Technology," J. of Soil and Water Conservation, Vol. 46, No. 1, pp. 34–38.

Lague D, Hovius N, Davy P. 2005. Discharge, discharge variability, and the bedrock channel profile, Journal of Geophysical Research, **110**: doi:10.1029/2004JF000259.

Lane, L., M. Nichols, L. Levick, and M. Kidwell, 2001, "A Simulation Model for Erosion and Sediment Yield at the Hillslope Scale," Chapter 8 (pp. 201-237) in Landscape Erosion and Evolution Modeling (Harmon, R. and W. Doe III, eds.), Kluwer Academic/Plenum Publishers, New York.

Lane, L., M., Wilson, C.J., Springer E.P., 2002. Field Data and Analysis of Event Based Surface Erosion: Initial Calibration of the 1000 Year Erosion Model For TA54, Materials Disposal Area (MDA) G. LA-UR-02-6257.

Lane, L.J., 2003, "White Paper Pertaining to The Role of Large Events in Determining Soil Erosion, Sediment Yield, and Rates of Landscape Evolution", Memo to LANL, January, 10 pp.

Larsen, I. J., L. H. MacDonald, E. Brown, D. Rough, M. J. Welsh, J. H. Pietraszek, Z. Libohova, J. de Dios Benavides-Solorio, and K. Schaffrath (2009), Causes of post-fire runoff and erosion: water repellency, cover, or soil sealing?, *Soil Science Society of America Journal*, *73*(4), 1393-1407. doi: 10.1080/07055900.2000.9649643.

Los Alamos National Laboratory (LANL), 2008, Performance Assessment and Composite Analysis for Los Alamos National Laboratory Technical Area 54, Area G, Revision 4, Los Alamos National Laboratory Report LA-UR-08-6764, October.

Molnar P, Anderson RS, Kier G, Rose J. 2006. Relationships among probability distributions of stream discharges in floods, climate, bed load transport, and river incision. *Journal of Geophysical Research* **111**: F02001, doi:10.1029/2005JF000310.

Moody, J. A., and D. A. Martin (2001), Post-fire, rainfall intensity–peak discharge relations for three mountainous watersheds in the western USA, *Hydrological processes*, *15*(15), 2981-2993. doi: 10.1002/hyp.386.

Moody, J. A., and B. A. Ebel (2012), Hyper-dry conditions provide new insights into the cause of extreme floods after wildfire, *Catena*, *93*, 58-63. doi: 10.1016/j.catena.2012.01.006.

Moody, J. A., and B. A. Ebel (2014), Infiltration and runoff generation processes in fire-affected soils, *Hydrological Processes*, *28*(9), 3432-3453. doi: 10.1002/hyp.9857.

Moody, J. A., D. A. Martin, S. L. Haire, and D. A. Kinner (2008), Linking runoff response to burn severity after a wildfire, *Hydrological Processes*, *22*(13), 2063-2074. doi: 10.1002/hyp.6806.

Moody, J. A., R. A. Shakesby, P. R. Robichaud, S. H. Cannon, and D. A. Martin (2013), Current research issues related to post-wildfire runoff and erosion processes, *Earth-Science Reviews*, *122*, 10-37. doi: http://dx.doi.org/10.1016/j.earscirev.2013.03.004.

Moody, J. A., B. A. Ebel, P. Nyman, D. A. Martin, C. Stoof, and R. McKinley (2016), Relations between soil hydraulic properties and burn severity, *International Journal of Wildland Fire*, *25*(3), 279-293. doi: 10.1002/2016WR019110.

Nyhan, J.W., Schofield, T.G. and Starmer, R.H., 1997. A water balance study of four landfill cover designs varying in slope for semiarid regions. *Journal of Environmental Quality*, *26*(5), pp. 1385-1392.

Reid, K.D., Wilcox, B.P., Breshears, D.D. and MacDonald, L., 1999. Runoff and erosion in a Piñon–Juniper woodland influence of vegetation patches. *Soil Science Society of America Journal*, *63*(6), pp. 1869-1879.

Sheppard, P.R., Comrie, A.C., Packin, G.D., Angersbach, K. and Hughes, M.K., 2002. The climate of the US Southwest. *Climate Research*, *21*(3), pp. 219-238.

Smith, R., D. Goodrich, D. Woolhiser, and C. Unkrich, 1995, "Chapter 20: KINEROS – A Kinematic Runoff and Erosion Model," in Computer Models of Watershed Hydrology, Singh, V. (ed.), Water Resources Publications, Highlands Ranch, Colorado, pp. 697–732.

Springer, E.P., 2004, Statistical Exploration of Matrix Hydrologic Properties for the Bandelier Tuff, Los Alamos, New Mexico, Los Alamos National Laboratory Report LA-UR-04-2830.

Stauffer, P.H., S. Chu, T.A. Miller, D. Strobridge, G. Cole, K.H. Birdsell, B.A. Robinson, C.W. Gable, D.E. Broxton, E.P. Springer, T.G. Shofield, 2013. Groundwater Pathway Model for the Los Alamos National Laboratory, Technical Area 54, Area G, Revision 1, LA-UR-13-24014.

Stone, J.J., L.J Lane, and E.D. Shirley, 1992, "Infiltration and Runoff Simulation on a Plane," Transactions of the American Society of Agricultural Engineers, Vol. 35, pp. 161–170.

Sveinsson, O. G., D. C. Boes, and J. D. Salas, 2001, "Population index flood method for regional frequency analysis", Water Resources Research, Vol. 37, No. 11, pp. 2733–2748.

Swetnam, T.W. and Betancourt, J.L., 1998. Mesoscale disturbance and ecological response to decadal climatic variability in the American Southwest. *Journal of Climate*, *11*(12), pp. 3128-3147.

Tarboton, D.G., 1997. A new method for the determination of flow directions and upslope areas in grid digital elevation models. Water resources research, 33(2), pp. 309-319.

Trenberth, K. E., A. Dai, R. M. Rasmussen, and D. B. Parsons (2003), The changing character of precipitation, Bulletin of the American Meteorological Society, *84*(9), 1205-1217. doi: 10.1175/BAMS-84-9-1205.

Tucker GE, Bras RL. 2000. A stochastic approach to modeling the role of rainfall variability in drainage basin evolution. Water Resources Research 36: 1953-1964.

Tucker, G.E. and Hancock, G.R., 2010. Modelling landscape evolution. Earth Surface Processes and Landforms, *35*(1), pp. 28-50.

Willgoose, G., 2005. Mathematical modeling of whole landscape evolution. Annu. Rev. Earth Planet. Sci., 33, pp. 443-459.

Willgoose, 2005, User Manual for SIBERIA, Telluric Research, Scone, NSW, Australia.

Willgoose, G. and S. Riley, 1998, "The Long Term Stability of Engineered Landforms of the Ranger Uranium Mine, Northern Territory, Australia: Application of a Catchment Evolution Model," Earth Surf. Process. Landf., Vol. 23, No. 3, pp. 237–259

Willgoose G.R., R.L. Bras, and I. Rodriguez-Iturbe, 1991a, "A coupled channel network growth and hillslope evolution model, I. Theory," Water Resources Research, Vol. 27, No. 7, pp. 1671–1684.

Willgoose G.R., R.L. Bras, and I. Rodriguez-Iturbe, 1991b, "A physical explanation of an observed link area-slope relationship," Water Resources Research, Vol. 27, No. 7, pp. 1697-1702.

Wilson, C.J., K.J. Crowell, and L.J. Lane, 2005, Surface Erosion Modeling for the Repository Waste Cover at Los Alamos National Laboratory Technical Area 54, Material Disposal Area G, Los Alamos National Laboratory Report LA-UR-05-7771, September.